EC Accepts, published online ahead of print on 17 November 2006
Eukaryotic Cell doi:10.1128/EC.00306-06

Radial mass density, charge, and epitope distribution in the *Cryptococcus neoformans* capsule

Michelle E. Maxson[1], Ekaterina Dadachova[1,2] Arturo Casadevall[1, 3*] and Oscar Zaragoza[1,4*]

Albert Einstein College of Medicine, Department of Microbiology and Immunology (1), Medicine (3) and Nuclear Medicine (2). 1300 Morris Park Avenue, Bronx, NY 10461

4) Present address: Servicio de Micología, Centro Nacional de Microbiología, Instituto de Salud Carlos III. Ctra. Majadahonda-Pozuelo Km 2. Majadahonda, Madrid 28220. Phone: +34918223661

* Arturo Casadevall and Oscar Zaragoza share senior authorship of this paper.

Keywords: *C. neoformans*, capsular polysaccharide, density, antibody, epitopes, capsule aging.

Running title: Structure of different radial regions of the *C. neoformans* capsule

Abbreviations: C3, complement protein 3; Dcb, diameter of the cell body; Dwc, Whole cell diameter; FITC, fluorescein-isothiocynate; GalXM, galactoxylomannan; GXM, glucuronoxylomannan; HVPC, hematocrit volume per cell; Ka, affinity constant; Sab, Sabouraud dextrose medium; SEM, scanning electron microscopy; TRITC, tetramethyl-rhodamine-isothiocynate; Vp, packed volume; Vwc, whole cell volume.

ABSTRACT

Exposure of *Cryptococcus neoformans* cells to γ-radiation results in a gradual release of capsular polysaccharide, in a dose dependant manner. This method allowed the systematic exploration of different capsular regions. Using this methodology, capsule density was determined to change according to the radial distribution of glucuronoxylomannan and total polysaccharide, becoming denser at the inner regions of the capsule. Scanning electron microscopy of cells following γ-radiation treatment confirmed this finding. The zeta potential of the capsule also increased as the capsule size decreased. However, neither charge nor density differences were correlated with any change in sugar composition (xylose, mannose and glucuronic acid) in the different capsular regions, since the proportion of these sugars remained constant throughout the capsule. Analysis of the capsular antigenic properties by monoclonal antibody binding and Scatchard analysis revealed fluctuations in the binding affinity within the capsule but not in the number of antibody binding sites, suggesting that the spatial organization of high and low affinity epitopes within the capsule changed according to radial position. Finally, evidence is presented that the structure of the capsule changes with capsule age, since the capsule of older cells became more resistant to γ-radiation-induced ablation. In summary, the capsule of *C. neoformans* is heterogeneous in its spatial distribution and changes with age. Furthermore, our results suggest several mechanisms by which the capsule may protects the fungal cell against exogenous environmental factors.

INTRODUCTION

Capsules are a common feature among microorganisms, especially pathogenic bacteria such as *Bacillus anthracis*, *Streptococcus pneumoniae, and Neisseria meningitides*. Microbial capsules can confer particular characteristics, such as protection against stress conditions (65), and are prominent virulence factors. In contrast to the situation in bacteria, extracellular capsules are rare in fungi. The only encapsulated pathogenic fungus is the basidiomycetes yeast *Cryptococcus neoformans*. This fungus is commonly found in the environment, inhabiting various nichés such as pigeon droppings, trees and water (reviewed in (9)). The pathogenesis of *C. neoformans* has been well studied. The yeast is commonly acquired by the host via inhalation. The infection is asymptomatic in immunocompetent hosts. However, in cases of immune suppression, pulmonary infection can be followed by extrapulmonary dissemination of the yeast into other organs, such as spleen, liver and brain. Untreated cryptococcal meningitis is invariably fatal.

The polysaccharide capsule of *C. neoformans* is considered the main virulence factor of this pathogen (38). Acapsular *C. neoformans* strains manifest greatly reduced virulence (11, 32), and mutants that produce a larger capsule are hypervirulent (16). The capsule of this yeast is believed to function in protection from desiccation, radiation, and predation by phagocytic organisms (reviewed in (10)). During pathogen-host interactions, the *C. neoformans* capsular polysaccharide is abundantly released into tissues (25), and has been associated with a myriad of deleterious immunological effects including antibody unresponsiveness (28, 48), inhibition of leukocyte migration (20), complement depletion (35), deregulation of cytokine production (54, 63, 64) and interference with antigen presentation (54). In addition, the capsular polysaccharide inhibits phagocytosis of the yeast by phagocytic cells (27, 71).

While the role of the *C. neoformans* capsule in virulence has been extensively studied, relatively little is known about the organization of this enigmatic structure. The capsule is composed of three basic elements, glucuronoxylomannan (GXM) representing 90-95% of the polysaccharide, galactoxylomannan (GalXM, 5%) and mannoproteins (less than 1%) ((53), reviewed in (5, 19, 39)). However, a recent study suggests that GalXM could be the major component in molar composition (41). All capsule-related structural studies have been based on analysis of GXM from capsular polysaccharide shed by *C. neoformans* (13). Shed GXM is

known to be a high molecular weight polysaccharide (1.7-7.3 MDa, depending on serotype) of complex structure (2, 3, 41, 59, 61). These studies also demonstrate that GXM contains six basic repeats of mannose chains that can be substituted in many combinations with xylose or glucuronic acid and organized fibers. The mannose backbone of the GXM can be *O*-acetylated, and this substitution is known to confer immunogenic characteristics (29, 40, 46). Although much work has focused on capsular exopolysaccharide, little is known about the nature of the polysaccharide retained on the *C. neoformans* cell. The capsule can be non-covalently attached to the cell body via the alpha-1,3-glucan of the cell wall (52). Recent findings have shown that the capsule is a dynamic structure, subjected to suffer changes according to the environment (see review in (42)). One peculiar feature of the *C. neoformans* capsule is that it changes in size according to environmental conditions (26, 62, 67, 69), and is dramatically enlarged upon interaction with mammalian hosts (4, 15, 22, 34, 56). Although there are several models for capsule growth (51), recent evidence supports the hypothesis that the capsule grows by apical enlargement, which may involve the addition of new fibers that attach to the existing polysaccharide through non-covalent bonds (41, 72). The spatial distribution of the capsular material is not equal throughout the capsule. Electron microscopy images and studies of penetration of fluorescently labeled-dextrans suggest that the capsule is denser in the regions close to the cell wall (24, 51).

In the early 1970's, it was described that extremely high doses of γ-radiation greatly reduced the size of the *C. neoformans* capsule (18), but this phenomenon was largely forgotten until recently, when it was rediscovered and examined in detail (7). Doses of γ-radiation that are thousands times lower than previously described (18) release capsular polysaccharide very efficiently, by a presumed mechanism involving the creation of free radicals from solution (7). This reaction occurs without affecting the viability of *C. neoformans*, which is γ-radiation resistant (7). In the present study, γ-radiation is utilized to investigate the structure of the *C. neoformans* capsule that is retained on the cell. Our results demonstrate quantitative and qualitative radial differences in polysaccharide composition, highlighting unsuspected complexity.

MATERIAL AND METHODS

Strains and growth conditions. *C. neoformans* strain H99 (serotype A) was used (50). This strain was selected because it is representative of the most prevalent pathogenic serotype, is a standard *C. neoformans* strain and provides a population with homogenous capsule and cell size during both log phase growth and capsule induction (69). In some experiments, the acapsular mutant *cap67* was used (11). The cells were routinely grown in Sabouraud dextrose media (Sab), at 30ºC with minimal shaking (150 r.p.m.). To induce capsule growth, cells were first grown overnight as described above, collected by centrifugation, washed three times in PBS (phosphate buffered saline) and counted using a hemocytometer. Then, cells were used to inoculate 10 mL of capsule inducing media (10% Sab in 50mM MOPS, pH 7.4 (67)) to a final concentration of $1x10^7$ cells/mL. Capsule induction was performed in 100 mm petri plates, incubated overnight at 37ºC without shaking. In some experiments, capsule enlargement was induced in 500 mL of inducing medium with moderate shaking (150 r.p.m.). Alternatively, to study the effect of cell age on capsule properties, cells were grown and induced as above, but in addition, cells were induced at 37ºC for 7 or 14 days. In some cases, prior to inoculation into capsule inducing media, the cell wall was labeled first in a solution of 4 mg/mL EZ link sulfo-NHS-LC-biotin in PBS (Pierce, IL) for 1 hr at room temperature at a cell density of $5x10^7$ cells/mL, extensively washed with PBS, and then placed in the capsule induction medium for the period of time indicated in the text. Biotinylated cells were detected using streptavidin-fluorescein-isothiocynate (FITC; 20 μg/mL; Biosource, Camarillo, CA).

γ-radiation treatment. Yeast cells with enlarged capsule were exposed to varying amounts of γ-radiation from radioisotope ^{137}Cs, to remove layers of the polysaccharide capsule by free radical attack. Briefly, capsule induced cells were washed three times in PBS to remove shed capsular polysaccharides, suspended in PBS or H_2O, and $5x10^7$ cells were radiated using the Shepherd Mark I Irradiator (JL Shepherd and Associates, San Fernando, CA) at the dose rate of 1388 rads/min. For all experiments, cells were irradiated for 0, 5, 10, 20, 30 or 40 minutes. Irradiated cells were collected by centrifugation. The supernatants containing shaved capsular polysaccharide were saved for analysis (see below). Radiated cells were washed three times in PBS and saved for analysis (see below). In a similar experiment, the cells were irradiated for 20

minutes, and centrifuged. The supernatant was kept at 4°C (0-20 minutes sample); meanwhile the cells washed with H_2O were resuspended in fresh H_2O, and irradiated for another 20 minutes. After this irradiation, cells were centrifuged and the supernatant collected (20-40 minutes sample).

India Ink staining and capsule size measurement. The *C. neoformans* capsule was visualized after suspension of the cells in India ink or by immunofluorescence using sulfo-NHS-LC-biotin / streptavidin-FITC labeling of the cell wall (see above) and 18B7 (5 μg/mL; (47)) / goat α-mouse-IgG1-tetramethyl-rhodamine-isothiocynate (TRITC; 5 μg/mL) labeling of the capsular edge. Samples were observed using an Olympus AX70 microscope, QCapture Suite V2.46 software for Windows, and Adobe Photoshop 7.0 for Macintosh. To calculate capsule relative size, the diameters of the whole cell, including capsule (D_{wc}), and cell body, limited by the cell wall (D_{cb}), were measured, using Adobe Photoshop 7.0 for Macintosh. The relative size of the capsule to that of the whole cell was defined, in percent, as $[(D_{wc} - D_{cb}) / D_{wc}] \times 100$. Twenty cells were measured for each determination, and the average and standard deviation calculated. In some cases, percent capsule volume after γ-irradiation (V_p) was also calculated from the volume (in μL) of cell-packing in hematocrit capillary tubes (37). Hematocrit volume per cell (HVPC) was calculated as V_p / number of cells. Percent capsule volume after γ-irradiation was defined as $(HVPC_{post\text{-}irradiation} / HVPC_{non\text{-}irradiated}) \times 100$. Alternatively, whole cell volume (V_{wc}) was calculated from immunofluorescence images, defined as $(4/3)\ \pi\ (D_{wc}/2)^3$. Capsule volume was defined as the difference between the volume of the cell with capsule and the volume of the cell. Percent capsule volume after γ-irradiation was calculated as $(V_{wc\ post\text{-}irradiation} / V_{wc\ non\text{-}irradiated}) \times 100$.

GXM measurement. Soluble GXM was measured by capture ELISA as in (8). Briefly, 96-well plates were coated with goat anti-mouse IgM (1 μg/mL, Southern Biotechnologies, Birmingham, AL) followed by capture antibody 2D10 (2 μg/mL, (47)). Samples were added and detected using primary mAb 18B7 (2 μg/mL, (47)) and secondary antibody goat α-mouse IgG1 conjugated to alkaline phosphatase (1 μg/ml, Southern Biotechnologies, Birmingham, AL). One mg/mL *p*-nitrophenyl phosphate dissolved in substrate buffer (1 mM $MgCl_2 \cdot 6H_20$; 50 mM

167 Na_2CO_3) was used for development, and absorbance measured at 405 nm, using a microplate
168 reader after incubation at room temperature for approximately 20 minutes.
169
170 **Total polysaccharide measurements**. The concentration of total polysaccharide was
171 determined in each of the γ-irradiated cryptococcal cell supernatants, using the phenol-sulfuric
172 acid colorimetric technique (21).
173
174 **Complement deposition on the *C. neoformans* capsule**. Complement (C3; complement
175 protein 3) deposition on the cryptococcal capsule was performed as in (71). Briefly, blood from
176 C57Bl/6J female mice (6-8 weeks old, National Cancer Institute) was obtained from the retro-
177 orbital cavity, and serum obtained after centrifugation. $2x10^7$ crytococcal cells were suspended in
178 700 µL freshly-obtained serum, and incubated at 37°C for 1 h. Cells were extensively washed,
179 and suspended in PBS. Samples containing 3 x 10^6 cells were γ-irradiated for 0, 5, 10, 20, 30 or
180 40 minutes, as described above. C3 was then detected using a FITC conjugated goat anti-mouse
181 C3 antibody (4 µg/mL, Cappel, ICN, Aurora, OH). To detect the capsular edge, monoclonal
182 antibody (mAB) 18B7 (10 µg/mL) was added, and detected using a TRITC conjugated goat anti-
183 mouse IgG1 antibody (10 µg/ml, Southern Biotechnology Associates, Inc, Birmingham, AL).
184 The cells were observed under fluorescent filters with the Olympus AX70 microscope, QCapture
185 Suite V2.46 software for Windows, and Adobe Photoshop 7.0 for Macintosh.
186
187 **mAb 18B7 protection of the *C. neoformans* capsule release**. A suspension of $5x10^6$
188 cyptococcal cells in 750 µL was incubated with either 0, 10, 50 100 or 500 µg/mL of mAb 18B7
189 for 1 hr. Cells were extensively washed, and suspended in PBS. Samples were then exposed to γ-
190 radiation for 20 minutes. mAb 18B7 that remained on the capsule was then detected using a
191 FITC conjugated goat anti-mouse IgG1 antibody (5 µg/mL). Cells were observed under
192 fluorescent filters with the Olympus AX70 microscope, QCapture Suite V2.46 software for
193 Windows, and Adobe Photoshop 7.0 for Macintosh.
194
195 **Scanning electron microscopy**. Approximately $5x10^7$ irradiated yeast cells were washed
196 in PBS three times and suspended in fixing solution (2% p-formaldahyde, 2.5% glutaraldehyde,

197 0.1M sodium cacolydate). Cells were then serially dehydrated with ethanol, coated with gold
198 palladium and visualized using a JEOL (Tokyo, Japan) JAM 6400 microscope.
199
200 **Measurement of Zeta potential**. Approximately $5x10^7$ yeast cells, were washed and
201 suspended in 1 mM KCl. Zeta potential measurements of the capsule surface were made using
202 the ZetaPlus zeta potential analyzer (Brookhaven Instruments, Holtsville, NY).
203
204 **Glycosyl composition analysis of supernatants from γ-irradiated cryptotococcal**
205 **cells**. Approximately $1x10^{10}$ cells with enlarged capsule were washed, suspended in dH_2O and γ-
206 irradiated for 0-20 minutes or 20-40 minutes as described above. Supernatant samples were
207 lyophylized, and analyzed for glycosyl composition at the Complex Carbohydrate Research
208 Center at University of Georgia (Atlanta, GA) (66). Analysis was performed on 0.2 mg of the
209 lyophylized samples by combined gas chromatography/mass spectrometry (GC/MS) of the per-
210 *O*-trimethylsilyl (TMS) derivatives of the monosaccharide methyl glycosides produced from the
211 sample by acidic methanolysis.
212
213 **Elemental analysis of material released from γ-irradiated cryptotococcal cells.**
214 Supernatants were prepared as described for the sugar composition analysis. Lyophilized
215 samples were then submitted to Quantitative Technologies, Inc. (Whitehouse, NJ) for
216 quantitative elemental analysis. C, H, O and N were measured by PE 2400 CHN Analyzer fitted
217 with an oxygen accessory kit. Samples were converted into gases by combustion, and product
218 gases separated by gas chromatography. The elemental percentages were detected by thermal
219 conductivity.
220
221 **Scatchard analysis.** Approximately $2x10^6$ γ-irradiated cells were incubated for 1 hour at
222 37ºC with 0.11, 0.22, 0.44, 0.66 or 0.88 nM ^{188}Re-18B7. Radioactivity of the treated samples
223 was counted in a γ-counter, the cells collected by centrifugation, and the radioactivity of the
224 pellets was counted in a γ-counter. Scatchard analysis (57), to compute the binding constant and
225 the number of binding sites per cell for 18B7, was performed as described previously (33).
226

Confocal microscopy and 3D reconstruction. Immunofluorescence was performed after labeling the capsule of induced $1x10^6$ cryptococcal cells with the following: calcofluor (50 µg/mL), FITC or TRITC conjugated 18B7 (3 µg/mL), and 12A1 or 13F1 (IgMs, (47), 10 µg/mL) followed by goat anti-mouse IgM conjugated to FITC or TRITC (5 µg/mL). Emission from 410-480 nm (calcofluor), 495-535 nm (FITC) and 566-648 nm (TRITC) was visualized using a Leica AOBS Laser Scanning Confocal. To obtain 3D images, z-series of each cell was obtained in 0.25µm slices, and 3D images processed with ImageJ (NIH) and Voxx (Indiana University) softwares.

RESULTS

Kinetics of capsule decrease after γ-radiation treatment. γ-radiation exposure of *C. neoformans* cells results in capsular polysaccharide release (7). This effect provided a means to study the radial composition of the capsule in a graded fashion. The capsule of *C. neoformans* strain H99 is normally 1-2 μm in diameter but the diameter increases to 5-8 μm under capsule induction conditions (69). Cryptococcal cells with the enlarged capsule were used for two reasons. First, a larger capsule size made it easier to observe different capsular regions and improved the visible resolution of the capsule so that changes after γ-radiation treatment. Second, capsule enlargement represents one of the first morphological changes that occur after host infection.

Capsule size gradually decreased as a function of irradiation time without affecting the size of the cell body, delimited by the cell wall (Figure 1A). Therefore, it is possible to expose several internal regions of the capsule by this method. The amount of radiation used to induce capsule release has no significant effect on cell viability (7). We then measured the relative size of the capsule compared with the size of the cell body. After each irradiation time, there was a significant reduction in the relative size of the capsule (Figure 1B, $p<0.002$ in all the comparisons). Around 70% of the capsule volume (data not shown) was released after 20 minutes of irradiation, and longer irradiation times (30 and 40 minutes) exposed inner regions that remain very close to the cell wall (about 1 μm distance). Subsequent immunofluorescence analysis showed that after 40 minutes of irradiation, some capsular polysaccharide still remained, as evidenced by mAb 18B7 binding (see below). However, using this method, several arbitrary layers of the capsule were exposed. Exposure of these layers, which differ in their distances from the cell wall, were dependent on the dose of γ-radiation (Figure 1C).

In interpreting our results, we considered the possibility that the observed decrease in capsule size was the result of an inner collapse mediated by γ-radiation, and not the release of the polysaccharide from the capsule exterior. To assess the mode by which γ-radiation released the cryptococcal capsule, the inner capsule was labeled with complement, by incubating the cells in serum, and then exposed the cells to γ-radiation. Complement (C3) binds to the polysaccharide capsule in the inner part of the capsule, in an interaction that is mediated by the formation of a

covalent bond linkage and can be easily observed by fluorescence (71, 72). We observed that when the cells were first placed in serum followed by irradiation, the signal produced by C3 was unaffected, remaining at a location close to the cell wall (Figure 2). Alternatively, we coated cells with varying amounts of mAb 18B7, followed by exposure to 20 minutes of γ-radiation. mAb 18B7 is known to bind to the outer regions of the cryptococcal capsule (71, 72). Immunofluorescence showed that at low antibody concentrations (10 μg/mL), irradiation resulted in decreased capsule size as well as release of bound mAb 18B7 (Figure 3). It is noteworthy that the binding of the Ab at these concentrations to the capsule did not change the size of this structure indicating that only γ-radiation was responsible for capsule size changes in our conditions. We did not use higher concentrations because they have been reported to deform the capsule (68). Therefore, exposure to γ-radiation results in a gradual release of the capsule which occurs at the capsule exterior, without affecting inner capsular regions.

During these experiments, we also observed that mAb 18B7-coated cells were more resistant to capsule shedding by γ-radiation, in a concentration dependent manner (Figure 3). The binding of 18B7 in antibody concentrations above 100 μg/mL completely prevented the release of the capsule measured by capsule size after India Ink staining (figure 3, see 20 minutes irradiation), which was confirmed by measurement of capsule relative size by India ink, and by capture ELISA to detect GXM in the supernatants of γ-irradiated cells (data not shown).

Polysaccharide density as a function of capsule radial distance. To study the polysaccharide density of the capsule, we first measured the volume released after different irradiation times by India Ink, and the amount of GXM (capture ELISA) or total polysaccharide (phenol sulfuric acid method) in the corresponding fractions. Significant amounts of GXM (figure 4A, black bars) and total polysaccharide (data not shown) were released after each irradiation time. However, this amount released did not correlate with the amount of volume lost by the cells (figure 4A, line). The density of the various capsular regions was then calculated (Figure 4B) from the amount of GXM released per cell (in μg), per volume (μm^3). The capsule GXM density was lowest at outer regions (~1.5 to 3 μm from the cell body), and dramatically increased at the inner regions (up to ~1.5 μm from the cell body). Interestingly, at the region closest to the cell wall, density decreased. This profile was also seen when total polysaccharide density was calculated (data not shown). The density profiles obtained from total polysaccharide

298 and GXM measurements were similar, strongly suggesting that the total polysaccharide content
299 in the capsule correlated with GXM concentration. These observations are consistent with data
300 indicating GXM is the major component of capsule mass. In addition, these results indicate that
301 polysaccharide distribution varies as a function of radial distance in the capsule.
302
303 **Structure of capsule layers observed by scanning electron microscopy.** We examined
304 γ-irradiated cells by scanning electron microscopy (SEM) to ascertain whether the measured
305 differences in density correlated with the visual appearance of the cells. We observed that γ-
306 irradiation exposed distinct regions of the capsule which differed in structural packing and
307 organization (Figure 5). Non-irradiated (untreated) cells appeared to be surrounded by two levels
308 of organized polysaccharide (see figure 5, time 0 panel). The outer capsule seemed to be a
309 diffuse web of fibers, while the inner capsule resembled a dense net. Irradiation for up to 20
310 minutes removed the outer layer, but did not affect the visually dense region, which is consistent
311 with the high density region predicted by calculation (see figure 4B). This tight network of
312 polysaccharide around the cell body differed from the capsule organization observed for cells
313 prior to capsule enlargement (un-induced). Comparisons to the *cap67* mutant, which lacks a
314 capsule, confirmed that even after 40 minutes of irradiation, some capsular polysaccharide
315 remained associated with the cell. These results are consistent with differential organization of
316 polysaccharide fibers according to their radial location in the capsule, although assumptions on
317 the nature of capsule structure based on electron microscopy must be made with caution. SEM
318 sample preparation requires serial dehydration, which may affect final capsule structure.
319 Regardless, the SEM data are consistent with the density calculations (see figure 4B), and
320 suggest that capsule enlargement is accompanied by a significant increase in the amount of
321 polysaccharide in the capsule.
322
323 **Charge distribution throughout the capsule.** *C. neoformans* cells are highly negatively
324 charged, due to the large amount of glucuronic acid present in the capsule. As a consequence, the
325 zeta potential obtained for non-encapsulated *C. neoformans* strains and other fungi is much lower
326 than for encapsulated cryptococcal cells (49). Consequently, we measured the zeta potential of
327 the cells after different doses of γ-irradiation (Fig. 6). Untreated cells had the lowest zeta
328 potential, at -37 mV. Zeta potential increased as a function of decreasing capsule thickness,

suggesting that the charge distribution is not equal throughout the capsule. In regions where the density was predicted to be higher, zeta potential did not significantly change.

Sugar composition and elemental analysis of the different polysaccharide fractions. To determine if the changes observed in polysaccharide density and charge were related to changes in the sugar composition of the capsular regions, the carbohydrate composition in the different polysaccharide fractions was analyzed. No significant differences were observed in the sugar composition of the different fractions (data not shown), but subtle differences in the molar ratios may have been masked by the large volume of capsule released in the first 20 minutes of irradiation. Therefore, we prepared two different fractions of the capsule by irradiating cells for 20 minutes, collecting supernatants, washing cells in H_2O and resuspending in new medium for 20 minutes further irradiation. We chose 0-20 minutes and 20-40 minutes, since the fractions obtained with these irradiation times corresponded to the low and high density regions of the capsule, respectively. However, no difference was detected in the sugar composition of the different fractions (Table 1). The presence of galactose indicates that GalXM is also released in the corresponding fractions. In addition, the elemental composition of the 0-20 minute and 20-40 minute fractions was analyzed for carbon, oxygen, nitrogen and hydrogen (Table 2). There was no difference in the proportion of these elements, a finding which is in agreement with the results obtained from the sugar composition. The relative paucity of nitrogen is consistent with a capsular structure composed almost entirely of polysaccharide with little or no protein. Concerning the sugar analysis, this was performed on supernatants from cells irradiated for 5, 10, 20, 30 and 40 minutes (without washes), and the results were the same (data not shown). The proportion of the elements measured is similar to the values obtained with purified GXM (McFadden, DC, personal communication) which confirms that most of the mass obtained from the capsule is GXM.

Antigenic properties of the different regions of the capsule. Given the apparent mass density and charge differences in the capsular layers, we evaluated changes in the antigenic structure of the *C. neoformans* capsule after graded exposure to γ-radiation. Previous studies used Scatchard analysis to calculate the number of binding sites and binding affinity (K_a) of the ^{188}Re labeled mAb 18B7 for the capsule after enlargement (17). We performed Scatchard

analysis using ^{188}Re labeled 18B7 for cells irradiated for 0, 10, 20, 30, 40 minutes (Table 3). Surprisingly, the number of binding sites and (K_a) showed that while the number of binding sites was equal throughout the capsule, the affinity of the antibody for the binding sites dramatically changed. The higher affinity binding sites for 18B7 were located at the outer and inner capsular regions (layers 1, 4 and 5). The central regions of the capsule (layers 2 and 3) had lower affinity binding sites.

The number of binding sites in the capsule remains relatively constant regardless of the irradiation time. In contrast, the mass density, charge and affinity of mAb 18B7 changed as a function of capsule radial distance. Therefore, we chose to evaluate whether the constant of number of binding sites represented an average of 18B7 binding throughout the capsule, skewed by binding at high affinity inner sites. When 18B7 binding was visualized by immunofluorescence using secondary antibodies, an annular binding pattern (71) was seen at the perimeter of the capsule and scanning electron micrographs showed a similar mAb cross-linking the capsule surface (14). To investigate if this was a consequence of the secondary mAb failing to penetrate the capsule surface, and to compare the results obtained from the Scatchard analysis, we visualized the distribution of 18B7 within the capsule, by using a mAb 18B7 directly conjugated to FITC and confocal microscopy. The cell wall of *C. neoformans* was labeled with calcofluor, and an IgM to GXM (12A1) was used to visualize the capsule edge. The fluorescence of each label was analyzed by confocal microsopy, and signal intensity plotted per μm distance (Figure 7).

MAb 18B7 distributed throughout the capsule, although a distinct gap of fluorescence was observed between the cell wall (calcofluor signal) and mAb 18B7. We also observed that there was a gap between the signal of 18B7 and the capsule edge, since the fluorescence of mAbs 18B7 and 12A1 did not co-localize at the capsule edge. The same results were obtained when we used a mAb 18B7 conjugated to TRITC, or when we detected capsule edge using mAb 13F1 (results not shown). Localization of mAb in the capsule by confocal microscopy was consistent with the idea that the number of binding sites seen from Scatchard analysis in non-irradiated cells and cells irradiated for 10 or 20 minutes includes binding sites in the inner capsule, although the binding sites exposed after 30 or 40 minutes most likely represents new epitopes that are not accessible initially by mAb 18B7 due to the high density of this region.

Cell age affects the susceptibility to γ-radiation. We observed that the amount of capsule released after γ-radiation was dependent on capsule age. In preliminary experiments, *C. neoformans* cells incubated for 7 or 14 days in capsule enlargement medium, seemed to become resistant to γ-radiation (Figure 8A). In these conditions, the size of the capsule did not significantly change after one day of incubation, as already reported (72). Capsule age could be an important factor when considering host infection and survival of the yeast in the environment. After irradiating cells 0, 20 or 40 minutes, the decrease in capsule size was measured (Figure 8B). After 7 and 14 days incubation, the capsule size of the population was heterogeneous; therefore, the average volume was measured using hematocrit tubes (37). This heterogeneity is most likely resulting from the limited period of budding that occurs in capsule enlargement media before nutrient exhaustion. The new buds generated do not have enough nutrients to build a capsule or grow in size. Nonetheless, when the decrease in capsule volume was measured as a percentage of the original capsule for overnight induced cells, and cells with 7 and 14 days induced capsule, the cells with 7 and 14 days induced capsule were increasingly more resistant to γ-radiation. This suggests that over time, changes occurred in the enlarged capsule of *C. neoformans,* that may be due to changes in the capsular structure and cross linking of GXM fibers.

A method to distinguish budded progeny from cells inoculated into the capsule inducing media was developed to enable a more precise analysis of the effect of capsule age on γ-radiation sensitivity. Cryptococcal cell wall was labeled with sulfo-NHS-LC-biotin prior to inoculation into capsule induction media. The biotin covalently binds to the cell wall, and does not segregate to the bud. In this way, the original inoculum of cells after incubation with TRITC conjugated streptavidin, and immunofluorescence was identified. After biotin labeling, cells were incubated overnight or for 7 days in capsule inducing media, and irradiated for 0, 20 or 40 minutes. The capsule edge was visualized by mAb 18B7 and detected by secondary antibody. Capsule size was measured on biotin-positive cells (Figure 9A). After 7 days incubation in inducing media, biotin-positive cells had a larger capsule size after γ-irradiation when compared to cells incubated overnight, measured by capsule volume percent decrease (Figure 9B) or by comparison of changes in capsule relative size (Figure 9C). The percent capsule decrease calculated here reproduced the values calculated using hematocrit volume measurements of the heterogeneous population (Figure 8B).

Finally, to get insight into whether there were structural differences between young and old induced capsule, we performed scanning electron microscopy on cells incubated in capsule inducing media for 7 days and irradiated for 0, 20 or 40 minutes (Figure 10, compared to figure 5). We observed the accumulation of a high density of polysaccharide fibers in a significant portion of the population throughout the capsule, when compared to overnight induced cells (Figure 10, figure 5). In addition, it was obvious that fibers on γ-irradiated cells were longer in length than those observed on overnight induced cells. This is another indication of γ-radiation resistance in older capsule cells.

DISCUSSION

γ-irradiation causes radiolysis of water resulting in short-lived free radicals that can react with polysaccharides and break glycosyl linkages (45, 58). Therefore, it is likely that capsule release following γ-irradiation occurs as a result of free radical attack on the capsule (7). Several lines of evidence discussed below suggest that this free radical attack only occurs on the outer surface. Cryptococcal cells labeled at the inner capsule by C3 did not show any changes in the organization of this region, as manifested by changes in the radial position of the C3 label. Although previous work had shown that γ-radiation exposure resulted in release of C3 binding region of the capsule (72), those studies involved cells with small, non-induced capsules where γ-radiation resulted in almost a total release of the polysaccharide. For cells with large induced capsule, C3 binds to the innermost layer, which is not released by γ-radiation. In a supporting experiment, we observe that coating of the capsule with mAb 18B7 conferred protection to γ-radiation to the capsule at high antibody concentration, while at lower concentrations the mAb is removed from the outer capsule by γ-radiation induced attack. Protection of the capsule from γ-radiation by antibody is consistent with the observation that antibody prevents polysaccharide shedding (36). In antibody coated cells, the immunoglobulin could quench free radicals produced by γ-radiation and reduce polysaccharide release by protecting the GXM. In this regard, the observation that antibody binding blocks the capsule release induced by free radicals could be an important consideration when studying the immunoregulatory effects of extracellular GXM during host infection. Overall, our results imply that the products of radiolysis formed after γ-radiation treatment react preferentially with capsule surface polysaccharides.

Capsule density varies dramatically at different regions of the capsule, with a trend for decreasing density as distance from the cell increases. Previous reports support these changes in density in the capsule (24, 51), although one account was based on mAb (Fab fragments) accumulation in the capsule (24), where it is possible that the penetration of the mAb to the inner regions was compromised. Our results give direct quantitative measurement of the polysaccharide distribution. When we compared capsule density with the results previously described in the literature we found consistent results (24), although our density values are higher than that reported. We think this difference is due to the experimental approach, since our

conditions (measurement of released GXM) presumably detect epitopes in GXM that are not accessible when the polysaccharide fibers are entangled within the capsule. The fact that independent experimental approaches gave consistent results confirms that capsule density varies as a function of the radial density. Interestingly, the density of the capsule peaked at about 1 μm from the cell and subsequently decreased at the most inner region, in agreement with micrograph images obtained after high-pressure freezing of the capsule (51). Although not understood, it is possible that this inner region is strongly attached to the cell wall, and plays an important role in stabilizing the capsule and providing a structural framework for the addition of new fibers in the higher density region. These changes in polysaccharide density after capsule enlargement support the current model of capsule growth, in which the newer fibers of polysaccharide intercalate between the existing ones, enlarging the capsule distally (41, 72). This model supports our observations because it predicts an increase in density proximal to the cell wall, where this intercalation would occur, and a decrease in density distal to the cell wall, where extension occurs. In addition, the higher density in the inner capsule offers an explanation for its increased resistance to γ-radiation. Our results are consistent with previous findings that revealed that the inner part of the capsule was more resistant to release by DMSO (24) or γ-radiation (6). This density distribution suggests a protective role during the interaction with the host, since it could prevent the penetration of molecules such as defensins and antibodies into the cell, on the basis of molecular size (24). Moreover, recent findings indicate that atypical India Ink penetration into the capsule does not permeate the inner high density regions of the capsule, instead forming an equatorial ring-like structure at the mid-capsule (70).

By exposing different regions of the capsule structural, differences in physical and antigenic properties were demonstrated. We observed changes in the zeta potential of the cells, decreasing as the radius of the capsule increased. This is in agreement with previous findings that showed a similar correlation between the zeta potential and capsule volume of different crytococcal strains with varying capsule size (49). We do not have a clear explanation for this result. The slight difference in the glucuronic proportion could be partially responsible for this effect. Zeta potential is the electrostatic potential of the area that surrounds the particle that it measured (55) and does not directly reflect the charge of the particle. The measured zeta potential is proportional to the charge of the particle, dependent on the dielectric constant and viscosity of the medium, and on the mobility of the particle. Since the medium remained the

same between samples, the difference in the zeta potential in the irradiated cells suggests dissimilarities the exposed capsule layers that affect the characteristics of the surface around the cells. Changes in zeta potential may have significance in host interactions, since they have been proposed/shown to affect the outcome of the phagocytosis (1, 60).

We also studied the antigenic properties of the different regions of the capsule by Scatchard analysis of mAb 18B7 binding to GXM. Our observations suggest that there is a great immunogenic variance within the capsule, and that there are high and low affinity binding sites present. To further understand the localization of this antibody, we analyzed the distribution of fluorescently conjugated mAb 18B7 by confocal microscopy, and showed that in fact this mAb localizes to the middle-outer regions of the capsule, but not to the region closest to the cell wall. The antibody is most likely unable to reach the epitopes at inner regions due to the increased density of the fibers, since these inner epitopes became available for antibody binding only after 30 and 40 minutes irradiation. Furthermore, antibody cross-linking of fibrils in the outer layers of the capsule may reduce penetration of subsequent molecules (68). This implies that for cells irradiated for less than 30 minutes, where the high density region of the capsule was unexposed, the determined number of binding sites is actually a measure of the binding sites in the entire low density capsule region. Intuitively, the actual number of binding sites per capsular region would only be a fraction of the total binding sites. This more closely correlates with the density trend. The localization of mAb 18B7 to the inner capsule, where there are epitopes with moderate high affinity, could represent a mechanism for immune evasion, since circulating antibodies would have to compete for binding at the capsule edge and interior. Binding at the latter location would render the antibody unavailable for Fc receptor binding on phagocytic and antigen presenting cells. All this together suggests that the difference in epitope distribution in the polysaccharide capsule could represent a relevant mechanism for the interaction between the pathogen and the host.

In addition to the differences in epitope distribution or organization, we found no significant differences in C, H, O proportions or in the sugar composition throughout the capsule. We found a trend toward decreasing glucuronic acid in regions closer to the cell wall. Previous reports (6) have described a difference in glucuronic acid, with this sugar being in significantly lower concentration in the inner regions of the capsule. Although our results might appear to be in discrepancy, the previous report used a combination of DMSO and γ-radiation to release the

523 capsule, a treatment that also removes the inner part of the capsule, a region that remains
524 attached to the cell in our conditions. In addition, DMSO can affect intracellular membranes and
525 release some intracellular polysaccharides, which could further alter the measured sugar
526 composition.

527 Finally, we have established that the susceptibility of cells to γ-radiation decreases with
528 capsule age. Our findings suggest that capsule age is associated with important changes in
529 capsular structure, in either cross-linking and/or in the amount of polysaccharide present in the
530 structure. This is a very significant finding, as the concept of capsule age is an important factor
531 during host infection. Previous reports show that after incubation in capsule inducing media, the
532 capsule grows in size but reaches a limit that correlates to cell size (72). The observations
533 presented here indicate that with age, the capsule no longer grows in size, but becomes denser by
534 accumulation of polysaccharide, as suggested by the SEM images. This implies that during *in*
535 *vivo* infection, where the fungal cells may stay in the lung for long periods of time, there are two
536 major changes that occur in the capsule. First, enlargement in size (early response), which occurs
537 during the first hours of infection (22), and second, increase in density and cross-linking (late
538 response), which would require several days. The first response would prevent phagocytosis of
539 the fungal cells by phagocytic cells present in the lung (30, 31, 44, 71). The second mechanism
540 would protect the fungal cells against the immune defense mechanisms found in the granulomas,
541 such as free radicals, that could damage the fungal cell. Our results have important implications
542 during the last stage, since increasing the amount of polysaccharide in the capsule could protect
543 the cell against a large number of molecules, such as free radicals, defensins or antibodies, or by
544 blocking penetration. In addition, it is known that the capsule suffers rearrangements *in vivo* to
545 allow for adaptation to different organs and crossing of the blood-brain-barrier (12, 23).
546 Furthermore, it has been described that prolonged incubation of *C. neoformans* in serum reduces
547 the reactivity of its capsular polysaccharide to mAbs (43), indicating that the capsule may
548 undergo rearrangements *in vivo* that allow for evasion of the host immune response, in this case,
549 by avoiding Ab binding.

550 The results of this study present a detailed study of several undefined aspects of the
551 cryptococcal capsule, the main virulence factor of this fungal pathogen. This structure is
552 heterogeneous and complex in its radial organization, and this complexity increases with capsule
553 age, as factors determining the amount and cross-linking of the polysaccharide fibers manifest.

This complex organization provides insight into the protective role of the capsule during interactions of *C. neoformans* with the host.

Acknowledgements. We are thankful to the Analytical Imaging Facility at Albert Einstein College of Medicine, especially to Michael Cammer, Rosana Leonard, Leslie Gunther**,** Clemenia Cayetano and Juan Jiménez for their great help in the preparation, observation and analysis of scanning electron micrographs, confocal images, and with 3D image reconstruction. We warmly thank Dr. Diane McFadden for communication of unpublished results, helpful discussions and for critical reading of the manuscript. We thank Dr. Bettina Fries and Emily Cook for useful technical suggestions. We thank Magdia De Jesus and Marcela Torres for the kind gift of the fluorescently-labeled mAb 18B7 and Ekaterina Revskaya for help with Scatchard measurements. Arturo Casadevall is supported by the following grants: AI33774-11, HL59842-07, AI33142-11, AI52733-02, GM 07142-01, and Ekaterina Dadachova is supported by the grant AI60507. The The glycosyl analysis was supported in part by the Department of Energy-funded (DE-FG09-93ER-20097) Center for Plant and Microbial Complex Carbohydrates.

REFERENCES

1. **Abbracchio, M. P., J. D. Heck, and M. Costa.** 1982. The phagocytosis and transforming activity of crystalline metal sulfide particles are related to their negative surface charge. Carcinogenesis **3:**175-180.
2. **Bacon, B. E., and R. Cherniak.** 1995. Structure of the O-deacetylated glucuronoxylomannan from *Cryptococcus neoformans* serotype C as determined by 2D 1H NMR spectroscopy. Carbohydr. Res. **276:**365-386.
3. **Bacon, B. E., R. Cherniak, K. J. Kwon-Chung, and E. S. Jacobson.** 1996. Structure of the O-deacetylated glucuronoxylomannan from *Cryptococcus neoformans* Cap70 as determined by 2D NMR spectroscopy. Carbohydr. Res. **283:**95-110.
4. **Bergman, F.** 1965. Studies on capsule synthesis of *Cryptococcus neoformans*. Sabouraudia **4:**23-31.
5. **Bose, I., A. J. Reese, J. J. Ory, G. Janbon, and T. L. Doering.** 2003. A yeast under cover: the capsule of *Cryptococcus neoformans*. Eukaryot. Cell **2:**655-663.
6. **Bryan, R. A., O. Zaragoza, T. Zhang, G. Ortiz, A. Casadevall, and E. Dadachova.** 2005. Radiological studies reveal radial differences in the architecture of the polysaccharide capsule of *Cryptococcus neoformans*. Eukaryot. Cell **4:**465-475.
7. **Bryan, R. A., O. Zaragoza, T. Zhang, G. Ortiz, A. Casadevall, and E. Dadachova.** 2005. Radiological studies reveal radial differences in the architecture of the polysaccharide capsule of *Cryptococcus neoformans*. Eukaryot. Cell **4:**465-475.
8. **Casadevall, A., J. Mukherjee, and M. D. Scharff.** 1992. Monoclonal antibody based ELISAs for cryptococcal polysaccharide. J. Immunol. Methods **154:**27-35.
9. **Casadevall, A., and J. R. Perfect.** 1998. *Cryptococcus neoformans*. ASM Press, Washington DC.
10. **Casadevall, A., J. N. Steenbergen, and J. D. Nosanchuk.** 2003. 'Ready made' virulence and 'dual use' virulence factors in pathogenic environmental fungi--the *Cryptococcus neoformans* paradigm. Curr. Opin. Microbiol. **6:**332-337.
11. **Chang, Y. C., and K. J. Kwon-Chung.** 1994. Complementation of a capsule-deficient mutation of *Cryptococcus neoformans* restores its virulence. Mol. Cell. Biol. **14:**4912-4919.
12. **Charlier, C., F. Chretien, M. Baudrimont, E. Mordelet, O. Lortholary, and F. Dromer.** 2005. Capsule structure changes associated with *Cryptococcus neoformans* crossing of the blood-brain barrier. Am. J. Pathol. **166:**421-432.
13. **Cherniak, R., and J. B. Sundstrom.** 1994. Polysaccharide antigens of the capsule of *Cryptococcus neoformans*. Infect. Immun. **62:**1507-1512.
14. **Cleare, W., and A. Casadevall.** 1999. Scanning electron microscopy of encapsulated and non-encapsulated *Cryptococcus neoformans* and the effect of glucose on capsular polysaccharide release. Med. Mycol. **37:**235-243.
15. **Cruickshank, J. G., R. Cavill, and M. Jelbert.** 1973. *Cryptococcus neoformans* of unusual morphology. Appl. Microbiol. **25:**309-312.
16. **D'Souza, C. A., J. A. Alspaugh, C. Yue, T. Harashima, G. M. Cox, J. R. Perfect, and J. Heitman.** 2001. Cyclic AMP-dependent protein kinase controls virulence of the fungal pathogen *Cryptococcus neoformans*. Mol. Cell. Biol. **21:**3179-3191.

17. **Dadachova, E., R. A. Bryan, C. Apostolidis, A. Morgenstern, T. Zhang, T. Moadel, M. Torres, X. Huang, E. Revskaya, and A. Casadevall.** 2006. Interaction of radiolabeled antibodies with fungal cells and components of immune system in vitro and during radioimmunotherapy of experimental fungal infection. J. Infec. Dis. **193:**1427-1436.
18. **Dembitzer, H. M., I. Buza, and F. Reiss.** 1972. Biological and electron microscopic changes in gamma radiated *Cryptococcus neoformans*. Mycopathol. Mycol. Appl. **47:**307-315.
19. **Doering, T. L.** 2000. How does *Cryptococcus* get its coat? Trends Microbiol. **8:**547-553.
20. **Dong, Z. M., and J. W. Murphy.** 1995. Effects of the two varieties of *Cryptococcus neoformans* cells and culture filtrate antigens on neutrophil locomotion. Infect. Immun. **63:**2632-2644.
21. **Dubois, M., K. Gilles, J. K. Hamilton, P. A. Rebers, and F. Smith.** 1951. A colorimetric method for the determination of sugars. Nature **168:**167.
22. **Feldmesser, M., Y. Kress, and A. Casadevall.** 2001. Dynamic changes in the morphology of *Cryptococcus neoformans* during murine pulmonary infection. Microbiology **147:**2355-2365.
23. **Garcia-Hermoso, D., F. Dromer, and G. Janbon.** 2004. *Cryptococcus neoformans* capsule structure evolution in vitro and during murine infection. Infect. Immun. **72:**3359-3365.
24. **Gates, M. A., P. Thorkildson, and T. R. Kozel.** 2004. Molecular architecture of the *Cryptococcus neoformans* capsule. Mol. Microbiol. **52:**13-24.
25. **Goldman, D. L., S. C. Lee, and A. Casadevall.** 1995. Tissue localization of *Cryptococcus neoformans* glucuronoxylomannan in the presence and absence of specific antibody. Infect. Immun. **63:**3448-3453.
26. **Granger, D. L., J. R. Perfect, and D. T. Durack.** 1985. Virulence of *Cryptococcus neoformans*. Regulation of capsule synthesis by carbon dioxide. J. Clin. Invest. **76:**508-516.
27. **Kozel, T. R., and E. C. Gotschlich.** 1982. The capsule of *Cryptococcus neoformans* passively inhibits phagocytosis of the yeast by macrophages. J. Immunol. **129:**1675-1680.
28. **Kozel, T. R., W. F. Gulley, and J. Cazin, Jr.** 1977. Immune response to *Cryptococcus neoformans* soluble polysaccharide: immunological unresponsiveness. Infect. Immun. **18:**701-707.
29. **Kozel, T. R., S. M. Levitz, F. Dromer, M. A. Gates, P. Thorkildson, and G. Janbon.** 2003. Antigenic and biological characteristics of mutant strains of *Cryptococcus neoformans* lacking capsular O acetylation or xylosyl side chains. Infect. Immun. **71:**2868-2875.
30. **Kozel, T. R., G. S. Pfrommer, A. S. Guerlain, B. A. Highison, and G. J. Highison.** 1988. Strain variation in phagocytosis of *Cryptococcus neoformans*: dissociation of susceptibility to phagocytosis from activation and binding of opsonic fragments of C3. Infect. Immun. **56:**2794-2800.
31. **Kozel, T. R., A. Tabuni, B. J. Young, and S. M. Levitz.** 1996. Influence of opsonization conditions on C3 deposition and phagocyte binding of large- and small-capsule *Cryptococcus neoformans* cells. Infect. Immun. **64:**2336-2338.

32. **Kwon-Chung, K. J., and J. C. Rhodes.** 1986. Encapsulation and melanin formation as indicators of virulence in *Cryptococcus neoformans*. Infect. Immun. **51:**218-223.
33. **Lindmo, T., E. Boven, F. Cuttitta, J. Fedorko, and P. A. Bunn, Jr.** 1984. Determination of the immunoreactive fraction of radiolabeled monoclonal antibodies by linear extrapolation to binding at infinite antigen excess. J. Immunol. Methods **72:**77-89.
34. **Love, G. L., G. D. Boyd, and D. L. Greer.** 1985. Large *Cryptococcus neoformans* isolated from brain abscess. J. Clin. Microbiol. **22:**1068-1070.
35. **Macher, A. M., J. E. Bennett, J. E. Gadek, and M. M. Frank.** 1978. Complement depletion in cryptococcal sepsis. J. Immunol. **120:**1686-1690.
36. **Martinez, L. R., D. Moussai, and A. Casadevall.** 2004. Antibody to *Cryptococcus neoformans* glucuronoxylomannan inhibits the release of capsular antigen. Infect. Immun. **72:**3674-3679.
37. **Maxson, M. E., E. Cook, A. Casadevall, and O. Zaragoza.** 2006. The volume and hydration of the *Cryptococcus neoformans* polysaccharide capsule. Fungal Genet. Biol. **in press**.
38. **McClelland, E. E., P. Bernhardt, and A. Casadevall.** 2006. Estimating the relative contributions of virulence factors for pathogenic microbes. Infect. Immun. **74:**1500-1504.
39. **McFadden, D. C., and A. Casadevall.** 2001. Capsule and melanin synthesis in *Cryptococcus neoformans*. Med. Mycol. **39 Suppl 1:**19-30.
40. **McFadden, D. C., and A. Casadevall.** 2004. Unexpected diversity in the fine specificity of monoclonal antibodies that use the same V region gene to glucuronoxylomannan of *Cryptococcus neoformans*. J. Immunol. **172:**3670-3677.
41. **McFadden, D. C., M. De Jesus, and A. Casadevall.** 2006. The physical properties of the capsular polysaccharides from *Cryptococcus neoformans* suggest features for capsule construction. J. Biol. Chem. **281:**1868-1875.
42. **McFadden, D. C., O. Zaragoza, and A. Casadevall.** 2006. The capsular dynamics of *Cryptococcus neoformans*. Trends Microbiol. **14:**497-505.
43. **McFadden, D. C., O. Zaragoza, and A. Casadevall.** 2004. Immunoreactivity of cryptococcal antigen is not stable under prolonged incubations in human serum. J. Clin. Microbiol. **42:**2786-2788.
44. **Mitchell, T. G., and L. Friedman.** 1972. In vitro phagocytosis and intracellular fate of variously encapsulated strains of *Cryptococcus neoformans*. Infect. Immun. **5:**491-498.
45. **Morelli, R., S. Russo-Volpe, N. Bruno, and R. Lo Scalzo.** 2003. Fenton-dependent damage to carbohydrates: free radicals scavenging activity of some simple sugars. J. Agric. Food. Chem. **51:**7418-7425.
46. **Moyrand, F., B. Klaproth, U. Himmelreich, F. Dromer, and G. Janbon.** 2002. Isolation and characterization of capsule structure mutant strains of *Cryptococcus neoformans*. Mol. Microbiol. **45:**837-849.
47. **Mukherjee, J., A. Casadevall, and M. D. Scharff.** 1993. Molecular characterization of the humoral responses to *Cryptococcus neoformans* infection and glucuronoxylomannan-tetanus toxoid conjugate immunization. J. Exp. Med. **177:**1105-1116.
48. **Murphy, J. W., and G. C. Cozad.** 1972. Immunological unresponsiveness induced by cryptococcal capsular polysaccharide assayed by the hemolytic plaque technique. Infect. Immun. **5:**896-901.

49. **Nosanchuk, J. D., and A. Casadevall.** 1997. Cellular charge of *Cryptococcus neoformans*: contributions from the capsular polysaccharide, melanin, and monoclonal antibody binding. Infect. Immun. **65:**1836-1841.
50. **Perfect, J. R., S. D. R. Lang, and D. T. Durack.** 1980. Chronic cryptococcal meningitis: a new experimental model in rabbits. Am. J. Pathol. **101:**177-194.
51. **Pierini, L. M., and T. L. Doering.** 2001. Spatial and temporal sequence of capsule construction in *Cryptococcus neoformans*. Mol. Microbiol. **41:**105-115.
52. **Reese, A. J., and T. L. Doering.** 2003. Cell wall alpha-1,3-glucan is required to anchor the *Cryptococcus neoformans* capsule. Mol. Microbiol. **50:**1401-1409.
53. **Reiss, E., M. Huppert, and R. Cherniak.** 1985. Characterization of protein and mannan polysaccharide antigens of yeasts, moulds, and actinomycetes. Curr. Top. Med. Mycol. **1:**172-207.
54. **Retini, C., A. Vecchiarelli, C. Monari, F. Bistoni, and T. R. Kozel.** 1998. Encapsulation of *Cryptococcus neoformans* with glucuronoxylomannan inhibits the antigen-presenting capacity of monocytes. Infect. Immun. **66:**664-669.
55. **Richmond, D. V., and D. J. Fisher.** 1973. The electrophoretic mobility of micro-organisms. Adv. Microb. Physiol. **9:**1-29.
56. **Rivera, J., M. Feldmesser, M. Cammer, and A. Casadevall.** 1998. Organ-dependent variation of capsule thickness in *Cryptococcus neoformans* during experimental murine infection. Infect. Immun. **66:**5027-5030.
57. **Scatchard, G.** 1949. The attraction of proteins for small molecules and ions. Ann. New York Acad. Sci. **51:**660-672.
58. **Sharpatyi, V. A.** 1999. Radiochemistry of polysaccharides. Radiat. Biol. Radioecol. **39:**156-161.
59. **Sheng, S., and R. Cherniak.** 1997. Structure of the 13C-enriched O-deacetylated glucuronoxylomannan of *Cryptococcus neoformans* serotype A determined by NMR spectroscopy. Carbohydr. Res. **301:**33-40.
60. **Tabata, Y., and Y. Ikada.** 1988. Effect of the size and surface charge of polymer microspheres on their phagocytosis by macrophage. Biomaterials **9:**356-362.
61. **Turner, S. H., R. Cherniak, E. Reiss, and K. J. Kwon-Chung.** 1992. Structural variability in the glucuronoxylomannan of *Cryptococcus neoformans* serotype A isolates determined by 13C NMR spectroscopy. Carbohydr. Res. **233:**205-218.
62. **Vartivarian, S. E., E. J. Anaissie, R. E. Cowart, H. A. Sprigg, M. J. Tingler, and E. S. Jacobson.** 1993. Regulation of cryptococcal capsular polysaccharide by iron. J. Infect. Dis. **167:**186-190.
63. **Vecchiarelli, A.** 2005. The cellular responses induced by the capsular polysaccharide of *Cryptococcus neoformans* differ depending on the presence or absence of specific protective antibodies. Curr. Mol. Med. **5:**413-420.
64. **Vecchiarelli, A., C. Retini, C. Monari, C. Tascini, F. Bistoni, and T. R. Kozel.** 1996. Purified capsular polysaccharide of *Cryptococcus neoformans* induces interleukin-10 secretion by human monocytes. Infect. Immun. **64:**2846-2849.
65. **Wilkinson, J. F.** 1958. The extracellualr polysaccharides of bacteria. Bacteriol. Rev. **22:**46-73.
66. **York, W. S., A. G. Darvill, M. McNeil, T. T. Stevenson, and P. Albersheim.** 1986. Isolation and characterization of plant cell walls and cell wall components. Methods Enzymol. **118:**3-40.

67. **Zaragoza, O., and A. Casadevall.** 2004. Experimental modulation of capsule size in *Cryptococcus neoformans*. Biol. Proced. Online **6:**10-15.
68. **Zaragoza, O., and A. Casadevall.** 2006. Monoclonal antibodies can affect complement deposition on the capsule of the pathogenic fungus *Cryptococcus neoformans* by both classical pathway activation and steric hindrance. Cell. Microbiol. **8:**1862-1876.
69. **Zaragoza, O., B. C. Fries, and A. Casadevall.** 2003. Induction of capsule growth in *Cryptococcus neoformans* by mammalian serum and CO(2). Infect. Immun. **71:**6155-6164.
70. **Zaragoza, O., E. E. McClelland, A. Telzak, and A. Casadevall.** 2006. Equatorial ring-like channels in the *Cryptococcus neoformans* polysaccharide capsule. FEMS. Yeast Res. **6**.
71. **Zaragoza, O., C. P. Taborda, and A. Casadevall.** 2003. The efficacy of complement-mediated phagocytosis of *Cryptococcus neoformans* is dependent on the location of C3 in the polysaccharide capsule and involves both direct and indirect C3-mediated interactions. Euro. J. Immnunol. **33:**1957-1967.
72. **Zaragoza, O., A. Telzak, R. A. Bryan, E. Dadachova, and A. Casadevall.** 2006. The polysaccharide capsule of the pathogenic fungus *Cryptococcus neoformans* enlarges by distal growth and is rearranged during budding. Mol. Microbiol. **59:**67-83.

FIGURE LEGENDS

Figure 1: Kinetics of capsule decrease after γ-radiation treatment. A) Cells from *C. neoformans* strain H99 with induced, large capsules were exposed to γ-radiation for 0, 5, 10, 20, 30 or 40 minutes, capsule size was observed by India ink staining of suspended cells. A representative cell from each time point was chosen to illustrate the effect of γ-radiation on capsule size. Scale bar, 10 μm. B) Capsule relative size from at least 20 cells was measured as indicated in Material and Methods. The average and the standard deviation of the relative size of the capsule are plotted. C) Schematic showing the capsular regions of *C. neoformans* strain H99 exposed after γ-irradiation.

Figure 2: Bound complement is unaffected by γ-radiation induced changes in capsule size. Cryptococcal cells with induced capsule were incubated in mouse serum to allow complement deposition on the capsule, which localizes and covalently binds to the inner capsule. Cells were then irradiated for 0, 5, 10, 20, 30 or 40 minutes, and immunofluorescence performed to detect complement localization (green fluorescence, FITC). To detect capsule edge, mAb 18B7 was added after the serum incubation, and then detected with GAM-IgG-TRITC. For each time point, upper left panel, light microscopy; upper right panel, rhodamine; lower left panel, FITC, and lower right panel, merge from both fluorescences. Scale bar, 5 microns.

Figure 3: γ-radiation of mAb-coated *C. neoformans* cells. Crytococcal cells with induced capsule were incubated with different concentrations of mAb 18B7. Cells were then irradiated for 20 minutes and compared to untreated cells. Immunofluorescence to detect 18B7 was performed using a GAM-IgG1-FITC Ab. The cells were suspended in parallel in India ink suspension to visualize the capsule. For each irradiation time: left column, cells suspended in India ink; middle column, light microscopy; right column, 18B7 localization, same field as the middle column. Note how cells present some aggregation, due to the "sticky" properties of Abs. Scale bar, 5 microns.

Figure 4: Polysaccharide density of the capsular layers. A) After γ-irradiation for 0, 5, 10, 20, 30 or 40 min, we calculated the total amount of GXM (grey bars) contained in each layer, per

cell (right axis), and compared this to the layer volume per cell (black line, and left axis). See Figure 1C for the spatial distribution of layers. B) Using the average amount of GXM per cell (Figure 4A) and the average volume per layer (Figure 1A), the average density of total GXM was calculated within the capsule regions. Experiment was duplicated with similar results, and one representative experiment presented.

Figure 5: Scanning electron microscopy of γ-radiation exposed capsule regions. Yeast cells with induced capsule were irradiated for 0, 5, 10, 20, 30 and 40 minutes, and then used to prepare samples for scanning electron microscopy. Scale bar of large panes, 5μm; scale bar of insets, 0.5 μm. Scanning electron micrographs of cells in which the capsule was not induced (H99 grown in Sab), and of the acapsular mutant *cap67* served as controls..

Figure 6: Zeta potential of the capsule after γ-irradiation. After irradiation for 0, 5, 10, 20, 30 or 40 minutes, the zeta potential of the exposed capsule was measured, and compared to capsule relative size, as determined by India ink staining. The average and standard deviation in a representative experiment is shown.

Figure 7: 18B7 epitope distribution in the *C. neoformans* capsule. Cells were γ-irradiated for 0, 20 or 40 minutes, then labeled with 18B7-FITC. The cell wall was detected using calcofluor, and the capsular edge detected by 12A1/GAM-IgM-TRITC . Pictures were taken using confocal microscopy. Panels show for each dose of γ-radiation (top to bottom): merged immunofluorescence labels, 3D reconstruction (ImageJ software), 3D Z-slice (VOXX software), 3D Z/Y-slice (VOXX), and fluorescent signal intensity profiles (ImageJ).

Figure 8: Effect of capsule age on capsule sensitivity to γ-irradiation. (A) After incubating crytococcal cells in capsule inducing conditions overnight, 7 days, or 14 days, cells were γ-irradiated for 0, 20 or 40 minutes, and the population observed by India ink staining. (B) The decrease in capsule size of cells, based on hematocrit cell packing, as a result of γ-irradiation for overnight (●), 7 days (■) or 14 days cultures (▲). The calculations were based on the percent volume of the 0 minute (untreated) sample. Average capsule volumes were measured by hematocrit cell packing.

Figure 9: Biotin labeling of *C. neoformans* cells to identify older cells, and quantify γ-radiation resistance. (A) Prior to induction, cells were labeled with EZ link sulfo-NHS-LC-biotin. After overnight or 7 days incubation in capsule inducing conditions, cells were γ-irradiated for 0 (untreated), 20 or 40 minutes, and the original inoculation detected with streptavidin-FITC. The capsular edge was detected using 13F1 and GAM-IgM-TRITC. Scale bar, 10 μm. (B) The decrease in capsule size of cells as a result of γ-irradiation, for overnight (●) and 7 day (◆) cultures. The calculations were based on the percent volume of the 0 minute (untreated) sample. The average capsule volumes were measured for biotin-positive cells. (C) Capsule relative size from at least 20 cells, for overnight (open bars) or for 7 day (closed bars) cultures, which were then irradiated for different periods of time. Capsule relative size was measured for biotin-positive cells, by immunofluorescence.

Figure 10: SEM comparison of young and old cells exposed to γ-radiation. *C. neoformans* cells were incubated overnight (upper row) or for 7 days (lower row) in capsule inducing conditions. Cryptococcal cells were then γ-irradiated for 0, 20 or 40 minutes and imaged by scanning electron microscopy. Scale bars, 5 μm.

TABLE 1. Glycosyl composition analysis of supernatants from γ-irradiated cryptococcal cells.

Glycosyl Residue	Mole percentage (%)[a]	
	0-20 minutes irradiated[b]	20-40 minutes irradiated[b]
Xylose (Xyl)	38.4	35.9
Glucuronic Acid (GlcA)	10.1	7.4
Mannose (Man)	34.7	32.1
Galactose (Gal)	5.6	4.5

[a] Values are expressed as mole percent of total carbohydrate. A representative experiment is shown.

[b] Exposure time of *C. neoformans* strain H99 to ^{137}Cs, which emits γ-radiation at the dose of 1388 rads/min.

TABLE 2. Qualitative elemental analysis of supernatants from γ-irradiated cryptococcal cells

Element	Weight Percentage[a]	
	0-20 minutes irradiated[b]	20-40 minutes irradiated[b]
Carbon	40	40
Hydrogen	6	6
Nitrogen	0.7	0.5
Oxygen	45	44

[a] Values are expressed as weight percentage of each element analyzed.

[b] Exposure time of *C. neoformans* strain H99 to ^{137}Cs, which emits γ-radiation at the dose of 1388 rads/min.

890 TABLE 3. Scatchard analysis of H99 capsular regions exposed by γ-radiation

Irradiation time[a]	K_a (x 10^7, M^{-1})[b]	Binding sites per cell (x 10^5)[b]
Untreated	29.0	5.9
10 minutes	4.9	7.0
20 minutes	5	7.4
30 minutes	12.0	4.6
40 minutes	8.0	7.3

[a] Exposure time of *C. neoformans* strain H99 to ^{137}Cs, which emits γ-radiation at the dose of 1388 rads/min.

[b] Determined by Scatchard analysis as described in (33). The experiment was done in duplicates, obtaining very similar results. A representative experiment is shown.

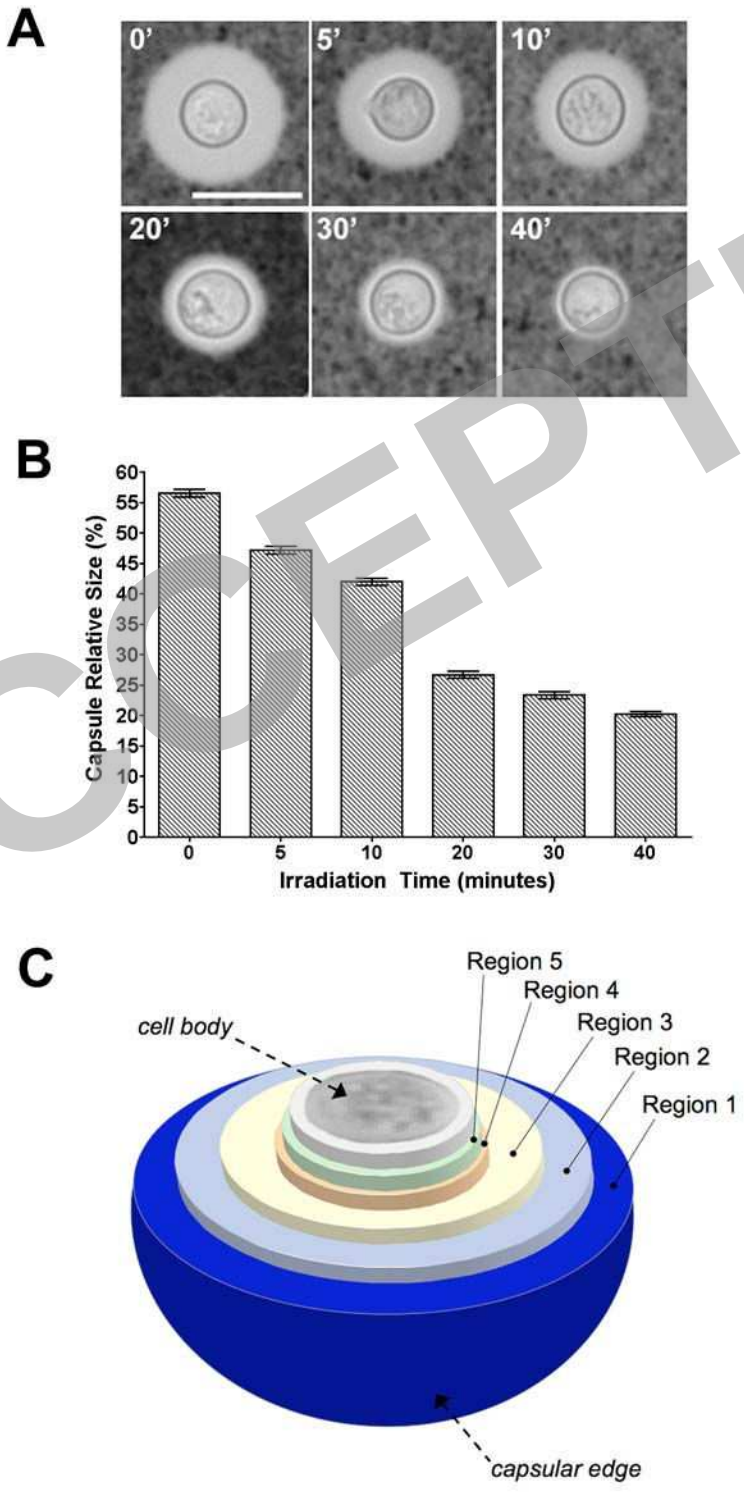

Figure 1

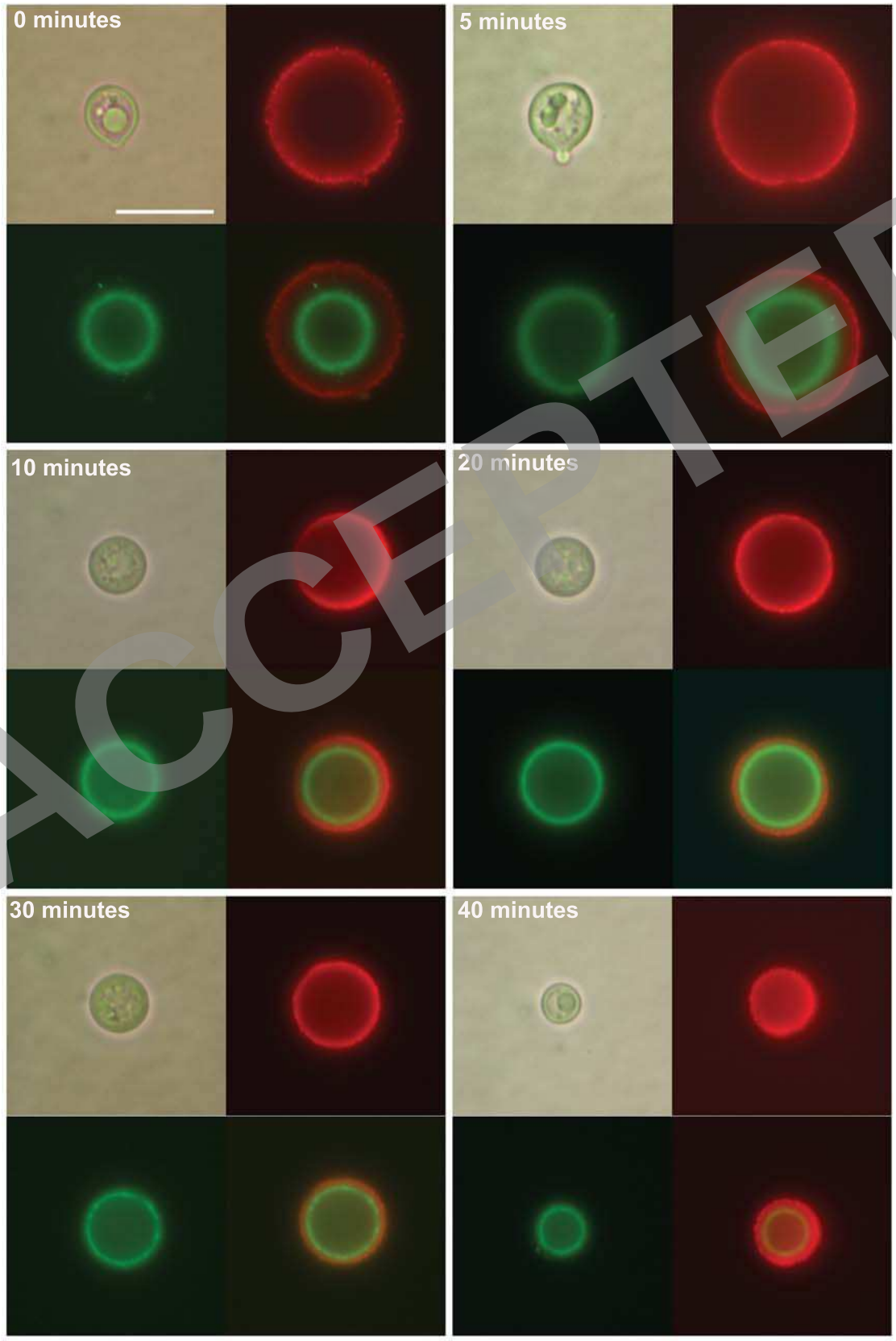

Figure 2

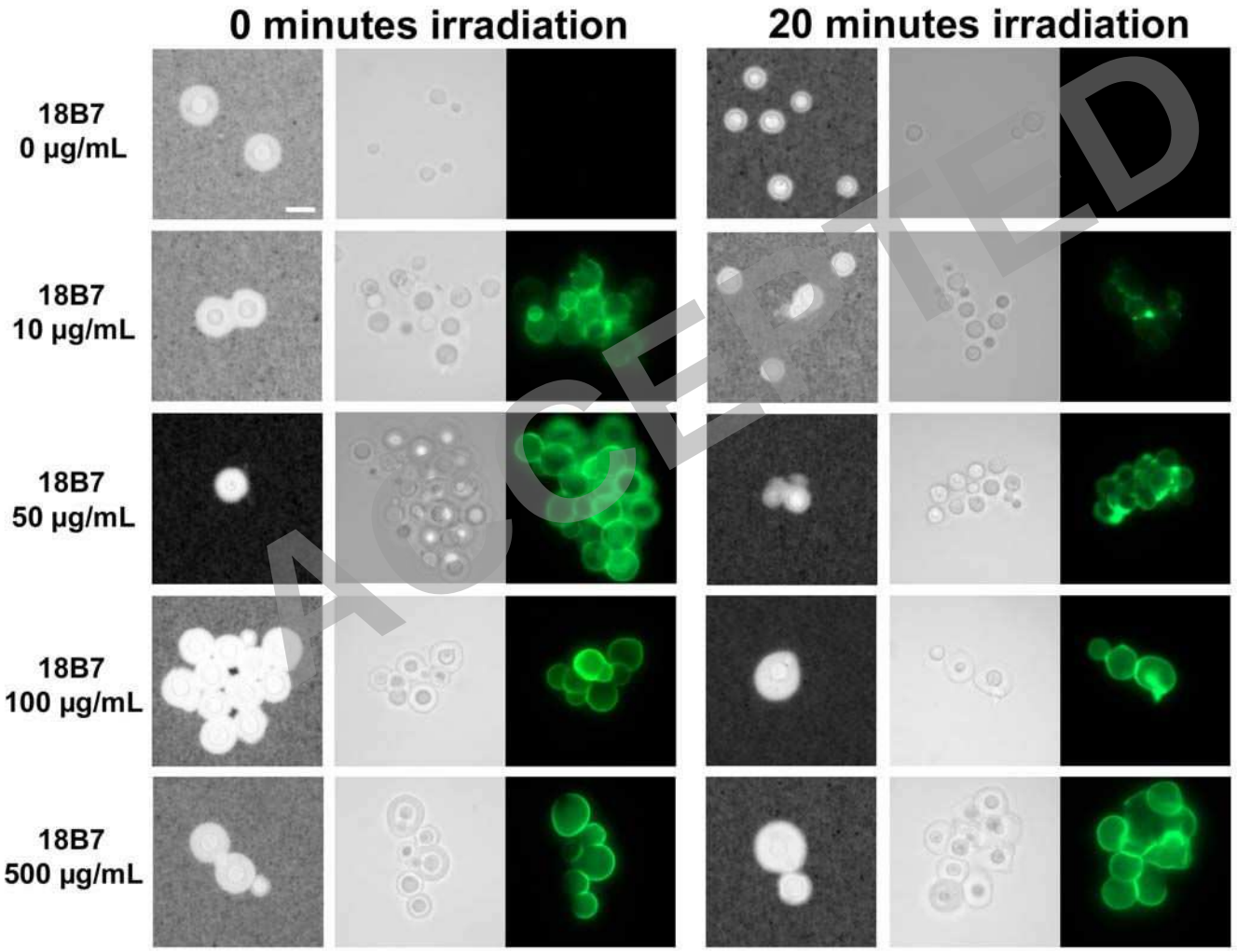

Figure 3

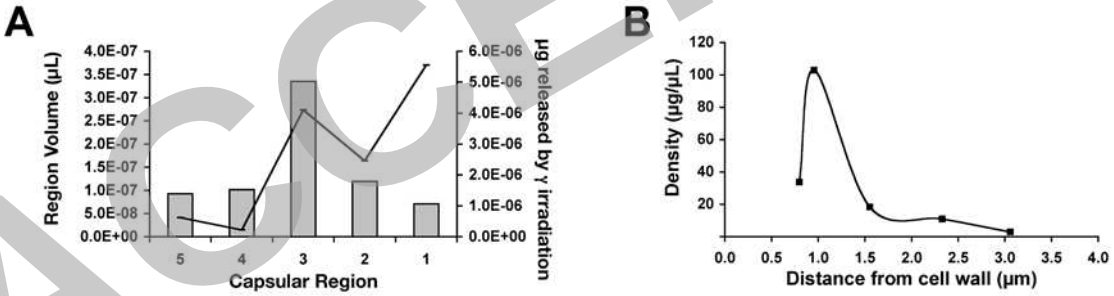

Figure 4

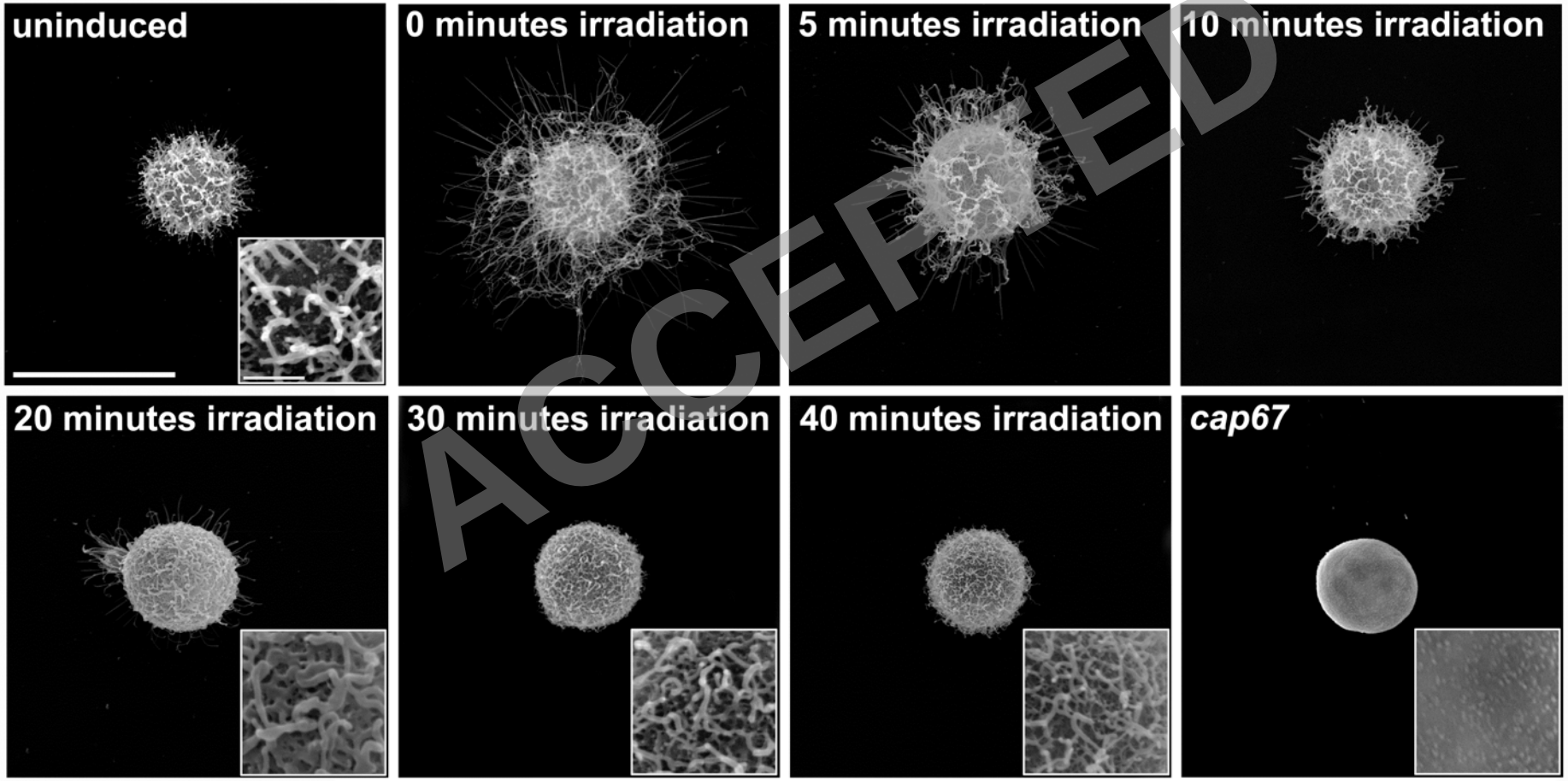

Figure 5

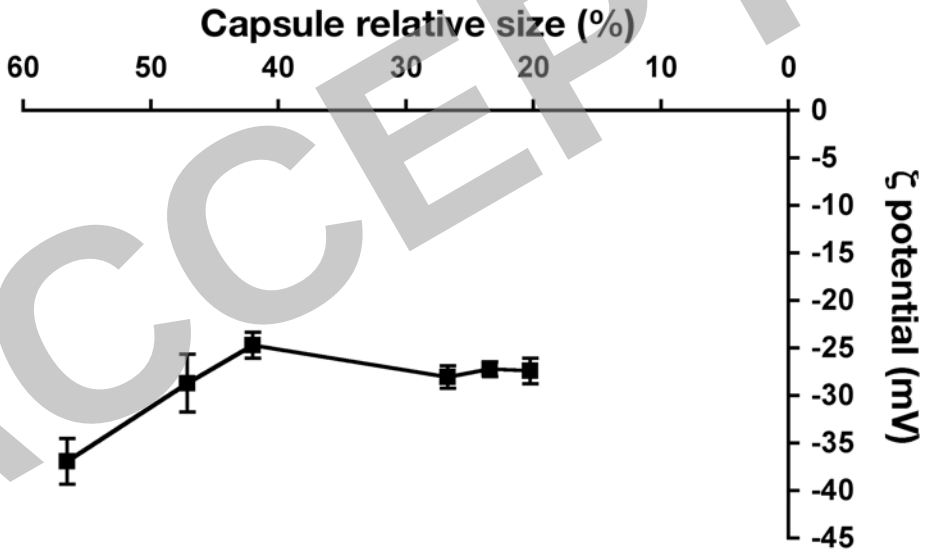

Figure 6

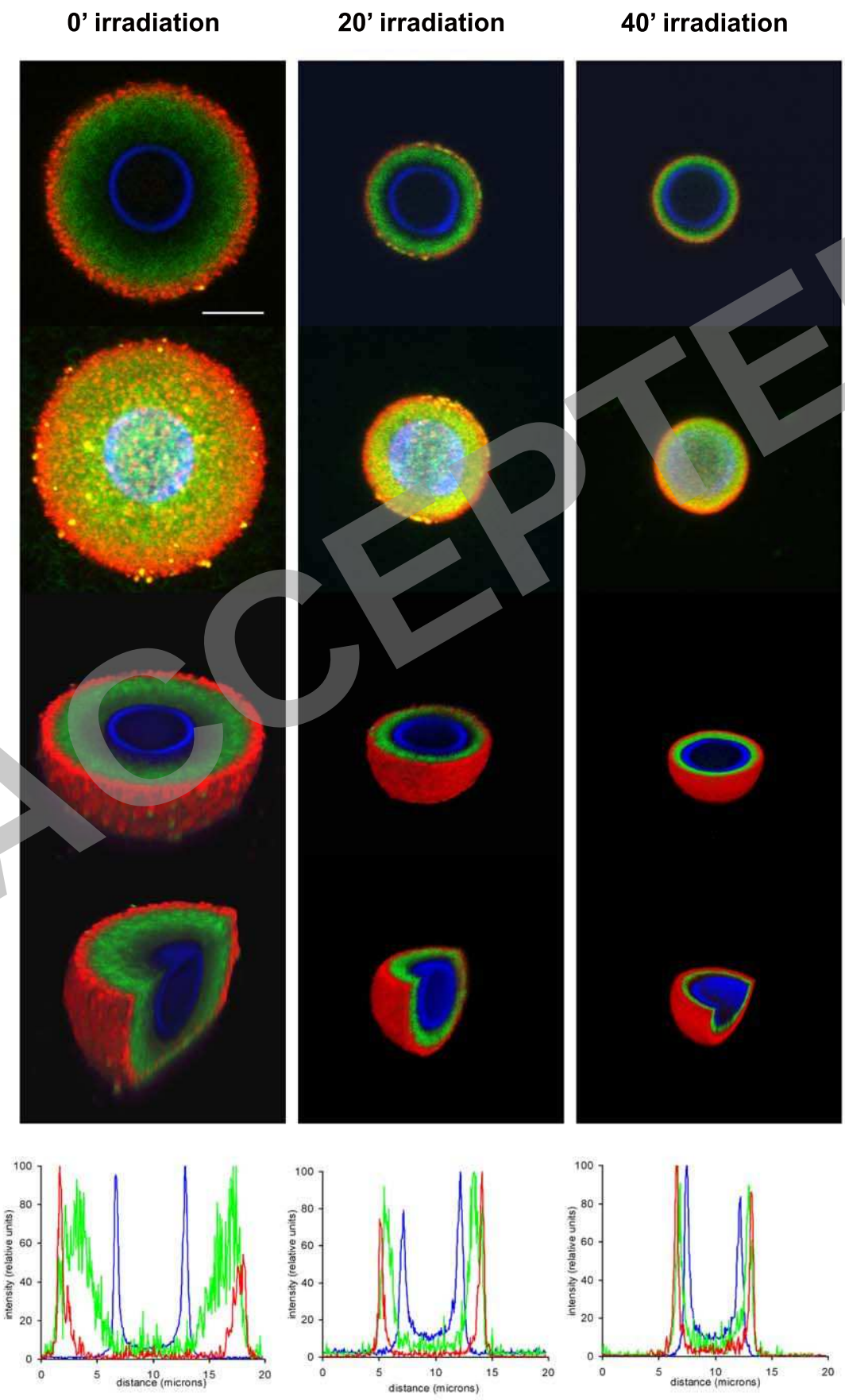

Figure 7

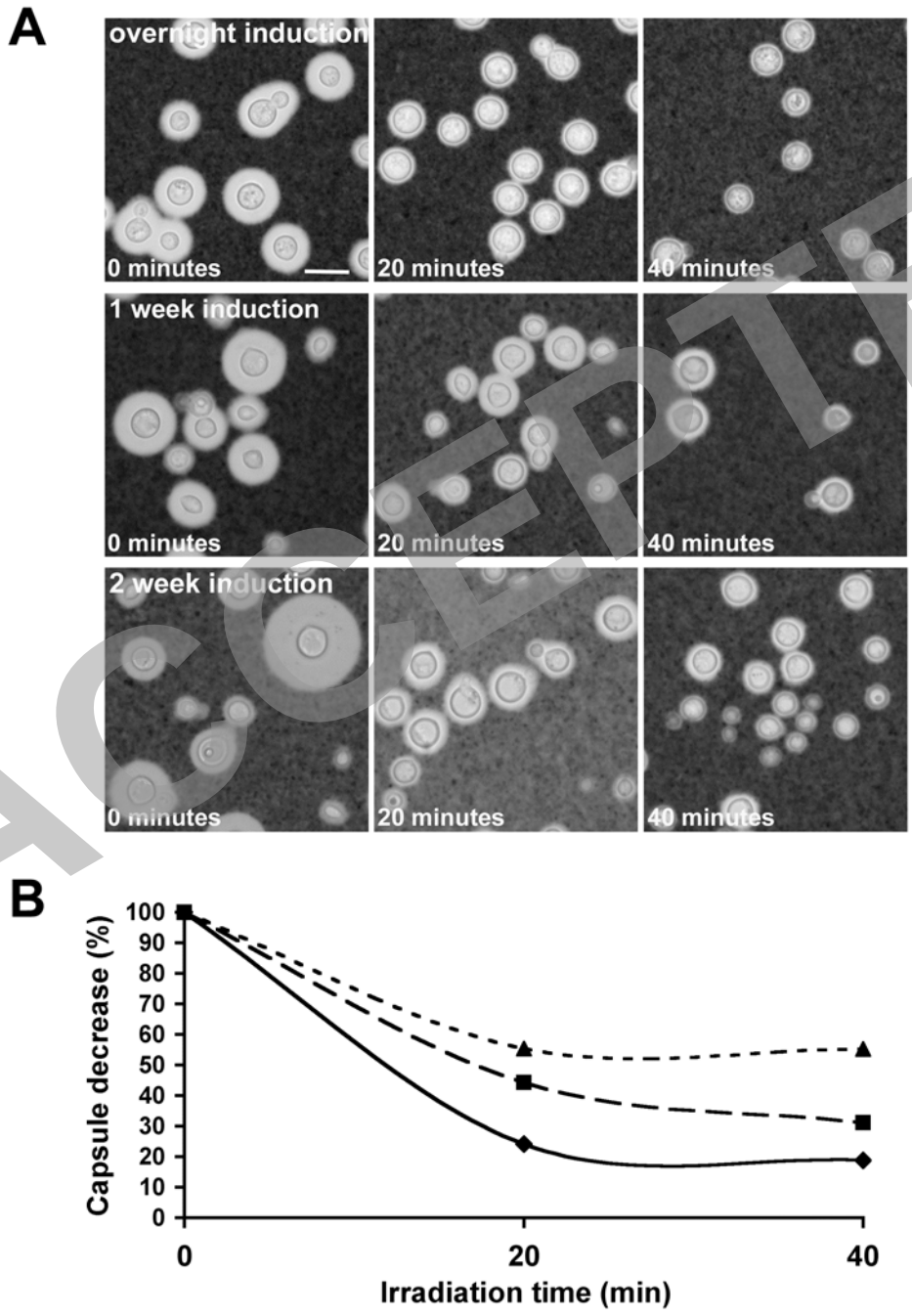

Figure 8

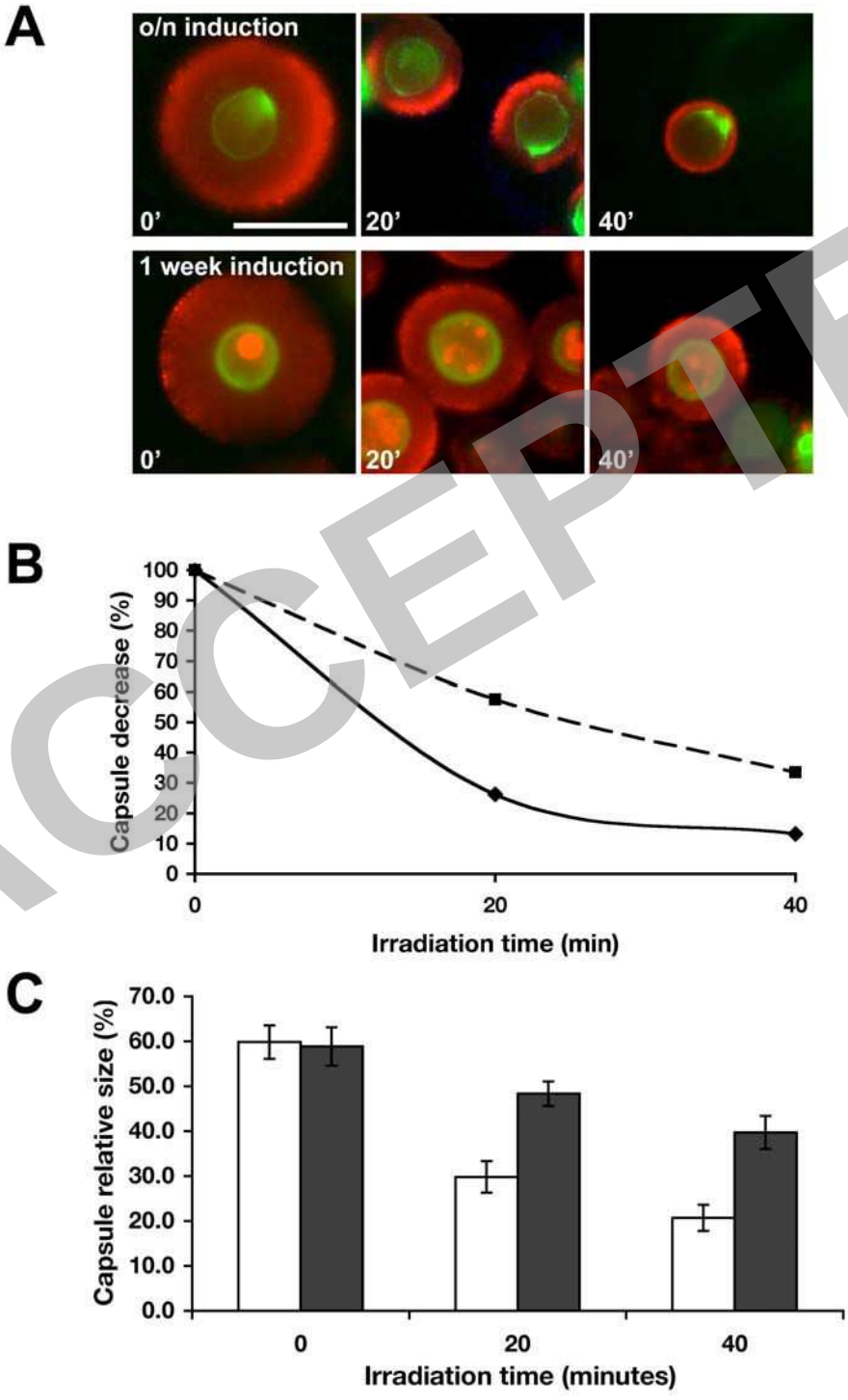

Figure 9

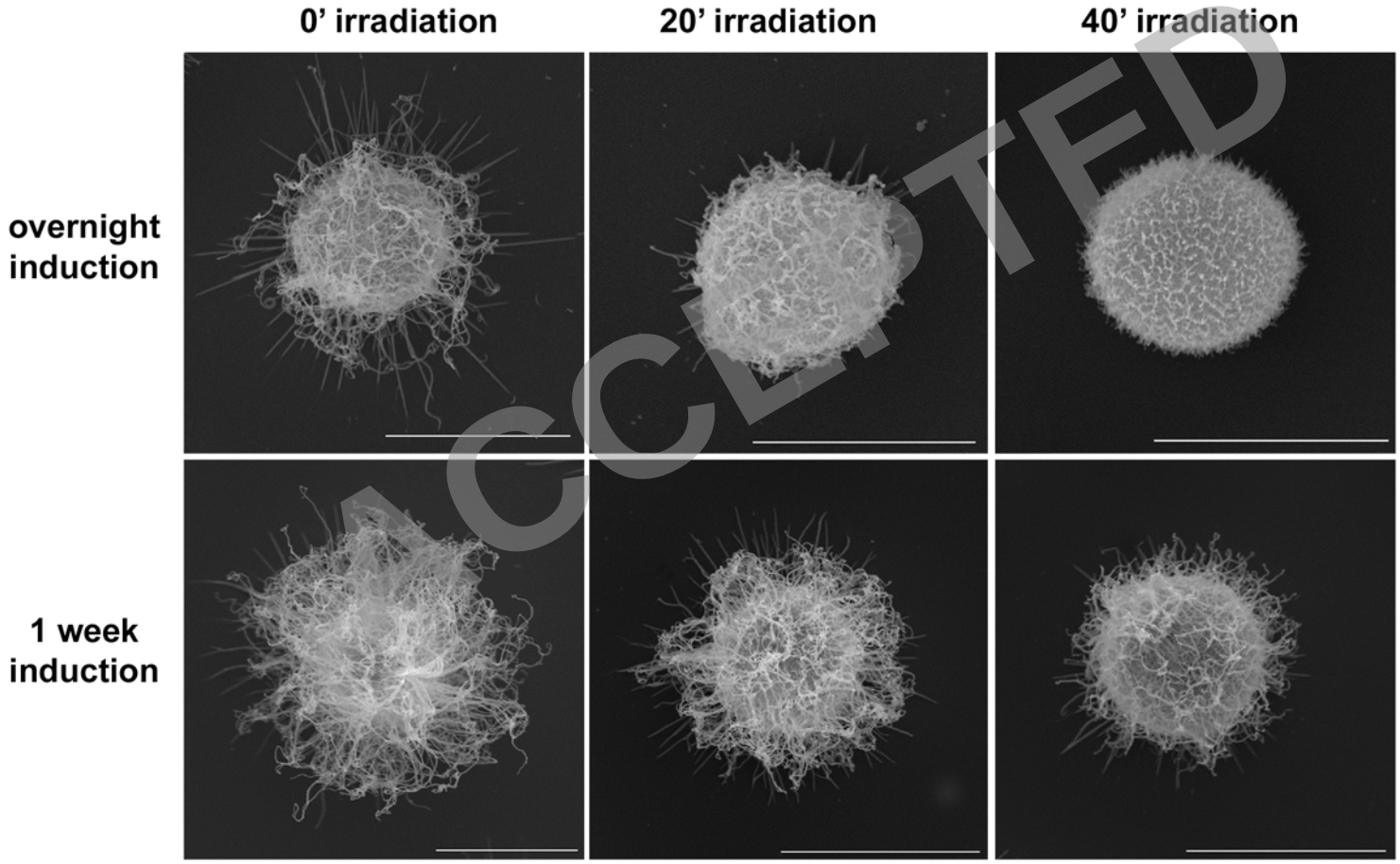

Figure 10